A Second-Order Lagrangian Macroscopic Traffic Flow Model for Freeways

Zhuoyang Zhou
Ph.D. Candidate
School of Computing, Informatics and Decision Systems Engineering
Arizona State University
Tempe, AZ 85281 USA
Email: zhuoyang.zhou.ie@gmail.com
Phone: 1-480-347-5436

Pitu Mirchandani
Professor
School of Computing, Informatics and Decision Systems Engineering
Arizona State University
Tempe, AZ 85281 USA
Email: pitu@asu.edu
Phone: 1-480-965-2758

Submitted to the
Symposium Celebrating 50 Years of Traffic Flow Theory
August 11-13, 2014

Please consider this article for publication in the special issue in Transportmetrica B or the Journal of Intelligent Transportation Systems.

ABSTRACT

A macroscopic traffic flow model describes the evolution of aggregated traffic characteristics over time and space, which is a basic and critical component for various modern intelligent transportation systems, e.g., a real-time freeway control system. Traditional macroscopic traffic flow models are built in the Eulerian coordinates using Eulerian traffic characteristics, such as density, speed and flow. Recently, the Lagrangian traffic flow modeling using Lagrangian traffic characteristics, such as spacing and speed, began to attract research attentions. It is favored over the Eulerian model mostly for its more accurate and simplified discrete simulation results (*1, 2*), and its convenience in incorporating vehicle-based information. However, up to now only a first-order model is presented (*1, 2*). Our paper proposes a new second-order Lagrangian macroscopic traffic flow model for freeways. The idea originates from Payne's second-order Eulerian model which was derived on the basis of car-following considerations (*3*). It reflects the fact that a driver usually adjusts the speed based on the traffic condition ahead, and that a time delay exists as a driver reacts to the changed traffic condition. A dynamic speed equation is formulated to represent these behavioral facts. A lane-drop scenario is simulated to examine the model performance. Comparison with the first-order Lagrangian model confirms the effectiveness and advantages of the proposed second-order model.

1 INTRODUCTION

For over sixty years, researchers have been devoting great efforts to model the complicated real world traffic flow system in mathematical ways. Macroscopic traffic flow modeling is a representative way to describe the evolution of aggregated traffic characteristics over time and space. The macroscopic models are widely applied in various modern intelligent transportation systems (ITS). For example, in real-time traffic state estimation, model-based traffic state estimators use macroscopic models to propagate aggregated traffic state variables over time and space.

According to the levels of detail, traffic flow modeling can be categorized into three levels. The lowest aggregated level depicting detailed individual driving behaviors is referred to as the *microscopic* traffic flow modeling, and the highest aggregated level focusing on the average traffic flow characteristics while neglecting the heterogeneous driving behaviors is referred as the *macroscopic* traffic flow modeling. *Mesoscopic* traffic modeling lies in between, digging into more details than the macroscopic models but still leaving out the detailed driving behaviors such as lane changing. Our research focuses on the macroscopic level.

With respect to coordinate systems, macroscopic traffic flow models can fall into either *Eulerian* models or *Lagrangian* models. The Eulerian coordinate system has its origin fixed in a spatial position, in which an observer standing on the freeway is stationary in this system while an observer riding on a vehicle is moving. In a Lagrangian coordinate system, the origin is fixed on the moving vehicles and thus any observer stationary to the freeway (stationary in the Eulerian coordinate system) is moving. The difference of the two systems lies in the change of observing perspectives. Typically, an Eulerian model defines state variables as locally aggregated traffic flow characteristics (traffic density, traffic flow, mean space speed), while a Lagrangian model uses vehicle group based characteristics (vehicle group position, vehicle group mean speed, vehicle group mean spacing). In this paper, we develop our model in the Lagrangian coordinate system, which is a relatively new and promising area.

Macroscopic traffic flow models can also be classified into *first-order* or *second-order* (or higher-order) models. The conservation equation and a fundamental diagram constitute a first-order model, while a second-order model incorporates an additional dynamic speed equation. In other words, the speed is no longer statically determined by the density/spacing condition according to the fundamental diagram. With the dynamic speed extension, researchers intend to elaborate the models on their capabilities in reproducing some of the real-world traffic patterns like oscillation in congestions, traffic hysteresis, and gradual speed change. In addition, the second-order model can be conveniently used in joint estimation of both density/spacing and speed at the same time in model-based real-time traffic state estimation, which further facilitates the utilization of speed measurements to enhance the estimation accuracy.

Traffic flow models may also have different emphasis on physical road conditions, e.g., freeways or local routes. Our proposed model assumes a freeway stretch.

There are several reasons motivate us to propose this second-order Lagrangian traffic flow model. (a) For empirical considerations, we believe that the reaction delay and anticipation should be reflected in the speed equation. (b) For practical considerations, this model would be a good candidate to conveniently incorporate vehicle-based spacing and speed information in model-based traffic state estimation. (c) For theoretical considerations, there are several existing Eulerian second-order models serving as a complementation to the first-order models. However, no such a model exists in the Lagrangian framework. Our model is the result of the efforts in bridging this gap.

For these purposes, a second-order Lagrangian macroscopic traffic flow model for freeways is proposed. In the rest of this paper, we first present an overview of existing traffic flow models in Section 2. Details of the proposed model are illustrated in Section 3. We evaluate the performance of this model in Section 4 through a simulation-based experimental analysis and conclude this paper in Section 5.

2 LITERATURE REVIEW AND MOTIVATIONS

A macroscopic traffic flow model generally includes (a) a conservation equation, and (b) a (static or dynamic) speed equation. This section reviews some popular existing Eulerian and Lagrangian traffic flow models.

Eulerian Traffic Flow Models

Traditional macroscopic traffic flow models are built in the Eulerian coordinate system. The Lighthill-Whitham and Richards (LWR) model (*4, 5*) is the most well-known model serving as the basis for most current macroscopic traffic flow models. It models the traffic flow dynamics as a kinematic wave model described by the partial differential equations below.

$$\begin{cases} \dfrac{\partial q(x,t)}{\partial x} + \dfrac{\partial \rho(x,t)}{\partial t} = 0 & (a) \\ q(x,t) = Q[\rho(x,t)] & (b) \end{cases} \tag{1}$$

Eq. 1-a is the conservation equation, stating that the change in flow (q) over space (x) equals to the change of density (ρ) over time (t) in the $x \times t$ space. Eq. 1-b is the fundamental diagram describing the nonlinear relationship between density and flow. Almost all of the macroscopic models are developed from this LWR model. For example, the widely applied Cell Transmission Model (CTM) (*6, 7*) is a discretized version of LWR with the assumption that the fundamental relationship between traffic flow and density is triangular. The freeway segment is discretized into a chain of fixed-length cells, assuming that the traffic condition within each cell is homogeneous. At each time step the traffic state variables are propagated along the spatial "cell-chain".

With specific formulation of the fundamental diagram and some numerical computation method, the LWR-type models can be implemented in discrete simulations. Plenty of research

has been conducted in this area to demonstrate the capabilities and drawbacks of the LWR-type models. It is demonstrated to be capable of reproducing basic phenomena observed in dynamic traffic flows in the real world, such as the conservation of vehicles, the forming and dissolving of congestion at bottlenecks, and the fact that the traffic condition is propagated over time and space in different directions under different prevailing traffic modes (e.g., congested or free flow) (*6, 8*). However, the main drawback of the LWR-type models is that vehicles are assumed to be able to attain their desired speed (represented by the fundamental diagram) instantaneously, implying infinite acceleration and deceleration. This problem and the resulted simulation inaccuracy lead the researchers to build higher-order models, mostly by incorporating a dynamic speed equation.

The second-order models assume that before vehicles reach the equilibrium speed described by the fundamental diagram, there is a time delay for acceleration or deceleration. For example, Payne (*3*) formulates the dynamic speed-density relationship as

$$v(x,t+\tau) = \mathrm{V}\left[\rho(x+\triangle x,t)\right] \tag{2}$$

Eq. 3 has the following assumptions: First, drivers adjust their speeds according to the downstream traffic condition, and thus the space mean speed $v(x,t)$ depends on the downstream density $\rho(x+\triangle x,t)$. Second, drivers gradually accelerate/decelerate in reaction to the traffic condition change ahead, that is, the desired (equilibrium) speed would be reached with a time delay (τ). Third, the dynamic speed relationship can be described by the Eulerian fundamental diagram with perturbations τ and $\triangle x$. Indeed, this model was derived on the basis of car-following considerations. Papageorgiou (*9*) extended the model to account for ramp flows. As we mentioned previously, the second-order models have been shown to be capable of reproducing traffic patterns where the first-order models are incapable of, and serving as a good candidate model for real-time traffic state estimations (*10*). However, there are also arguments questioning the reasonability of the high-order models. Daganzo (11) criticizes the possibility of negative flow and speed prediction in some extreme conditions. Others have noticed the underlying assumption that the desired speed distribution is a property of the road but not the drivers (*12*). Papageorgiou (*13*) argues that the second-order models have their merits in remedying the false assumption of the static fundamental diagram, and that the negatively predicted flow/speed values occur only in extreme conditions. Other common blames include that the second-order models have more parameters to be calibrated, and that the stability requirement becomes stronger in discrete simulation. Fortunately, these difficulties can be successfully overcome with careful model calibration efforts. As we see more and more second-order models in ITS applications in recently years, we believe that the advantages of the second-order models cannot be dismissed.

Lagrangian Traffic Flow Models

Originating from the flow dynamics theory, macroscopic flow movement can also be observed in the perspective of a moving particle in the flow, which defines the Lagrangian coordinate system. Leclercq (*1*) presented the formulation of the LWR PDE model in Lagrangian coordinates:

$$\begin{cases} \dfrac{\partial s(n,t)}{\partial t} + \dfrac{\partial u(n,t)}{\partial n} = 0 & (a) \\ u(n,t) = U[s(n,t)] & (b) \end{cases} \tag{3}$$

The first Eq. 2-a is the Lagrangian conservation equation. It states that the change of spacing (s) over time equals to the change of the mean speed (u) over the cumulative of number of vehicles (n) in the $n \times t$ space. This Lagrangian conservation equation can be derived from the Eulerian conservation equation by applying $s = 1/\rho$, $q = \partial n / \partial t$ and $\rho = -\partial n / \partial x$ (*1*). The second Eq. 2-b is the Lagrangian fundamental diagram, a function relating the spacing to speed, which can be obtained by applying $s = 1/\rho$ to the Eulerian fundamental diagram. An examples of the Lagrangian fundamental diagram is the Smulders' fundamental diagram (*14*):

$$u = U(\mathrm{s}) = \begin{cases} v_f - s_{cr} \cdot \dfrac{v_f - v_{cr}}{s}, & \text{if } s \geq s_{cr} \\ v_{cr} \cdot \dfrac{s - s_{jam}}{s_{cr} - s_{jam}}, & \text{otherwise} \end{cases} \tag{4}$$

where v_f, v_{cr}, s_{cr}, and s_{jam} stand for the free flow speed, the critical speed, the critical density, and the jam density, respectively. Another example is an exponential-form fundamental diagram (*9*) in Eq. 5, where a is a parameter needs calibration.

$$u = U(\mathrm{s}) = \mathrm{v}_f \cdot \exp\left[-\frac{1}{a} \left(\frac{s_{cr}}{s} \right)^a \right] \tag{5}$$

Van Wageningen-Kessels (*2*) develops a concrete framework for implementing the first-order Lagrangian traffic flow model for mixed-class and multi-class vehicles. In the mixed-class model, the traffic flow is discretized into vehicle groups using Godunov scheme. The advantages of this alternative to the traditional Eulerian models can be summarized as following. First, the traffic characteristics are propagated only in the flow direction since drivers only react to the front vehicles, which simplifies the discretization procedure (the upwind method). Second, the discrete simulation results show higher accuracy in many scenarios, compared with the Eulerian case. Third, the vehicle-based information (e.g., spacing measurements) can be directly used in state estimation (*15*). Since the Lagrangian modeling is a relatively new area, no second-order traffic flow model has been presented yet.

3 A SECOND-ORDER LAGRANGIAN MODEL

Applying the same idea as Payne's (*3*), we start our modeling with the following dynamic speed equation:

$$u(n,t+\delta_t) = U[s(n-\delta_n,t)] \tag{6}$$

Eq. 6 has the following three assumptions. First, the speed is adjusted according to the traffic condition ahead. As n stands for the accumulated volume of vehicles, it is decreasing along the flow direction, and $(n-\delta_n)$ corresponds to a position in the downstream ($\delta_n > 0$). Second, the speed is gradually changing with finite acceleration/deceleration, and the equilibrium speed cannot be reached until δ_t time later. Third, the dynamic speed relationship can be described by the spacing-speed fundamental diagram with perturbations δ_n and δ_t.

Derivation of the Dynamic Speed PDE

Expanding the right side of Eq. 6 using Taylor expansion, we obtain Eq. 7.

$$\begin{aligned} u(n,t) + \delta_t \cdot \frac{\mathrm{d}u(n,t)}{\mathrm{d}t} &= U[s(n,t)] - \delta_n \cdot \frac{\mathrm{d}U[s(n,t)]}{\mathrm{d}n} \\ &= U[s(n,t)] - \delta_n \cdot \frac{\partial U[s(n,t)]}{\partial s(n,t)} \cdot \frac{\partial s(n,t)}{\partial \mathrm{n}} \end{aligned} \tag{7}$$

We apply the following assumptions that are similar to those in the Eulerian models. Assume $\delta_n = \theta \cdot \rho = \theta / s$, where θ is a constant parameter assumed to be around $\theta = 0.5$. Assume that $\partial U[s(n,t)] / \partial s(n,t)$ is positively constant. Let $\lambda = \theta \cdot \frac{\partial U[s(n,t)]}{\partial s(n,t)}$, and the right-hand side of the Eq. 7 becomes $U[s(n,t)] - \frac{\lambda}{s} \cdot \frac{\partial s(n,t)}{\partial \mathrm{n}}$.

The term $\frac{\mathrm{d}u(n,t)}{\mathrm{d}t}$ in Eq. 7 is the acceleration term which should be treated as $\frac{\mathrm{d}u(n(t),t)}{\mathrm{d}t}$, leading to Eq. 8.

$$\frac{\mathrm{d}u(n(t),t)}{\mathrm{d}t} = \frac{\partial u}{\partial t} + \frac{\partial u}{\partial n} \cdot \frac{\partial n}{\partial t} \tag{8}$$

Applying $\partial n / \partial t = q = u / s$ and letting $\tau = \delta_t$, we finally obtain the dynamic speed PDE in Eq. 9.

$$\frac{\partial u(n,t)}{\partial t} = -\frac{\partial u(n,t)}{\partial n} \cdot \frac{u(n,t)}{s(n,t)} + \frac{1}{\tau} \cdot \left[U[s(n,t)] - u(n,t) - \frac{\lambda}{s} \cdot \frac{\partial s(n,t)}{\partial \mathrm{n}} \right] \tag{9}$$

Eq. 3-a, Eq.9, and a fundamental diagram (e.g., Eq. 4/Eq. 5) constitute the proposed continuous second-order Lagrangian traffic flow model.

Discrete Model

Let j be the index for the vehicle group and $j=1$ represents the vehicle group in the most downstream, and k be the index for the time steps. Let Δn denote the vehicle group size over all lanes, and let η_j denote the vehicle group size per lane. Thus $\eta_j = \frac{\Delta n}{L_j}$ and $\partial n = -\eta_j$. Note that in the macroscopic level n is a continuous dimension, and thus Δn is continuous as well. ε is added to the denominator to ensure computation stability. The discretized model consists of the following three equations.

$$\begin{cases} s_j(k+1) & = s_j(k) + \frac{T}{\eta_j} \cdot \left[u_{j-1}(k) - u_j(k) \right] \\ u_j(k+1) & = u_j(k) + \frac{T}{\tau} \cdot \left[U(s_j(k)) - u_j(k) \right] + \frac{T}{\eta_j} \cdot \frac{u_j(k)\left[u_{j-1}(k) - u_j(k) \right]}{s_j(k) + \varepsilon} + \frac{T\lambda}{\tau \eta_j} \cdot \frac{\left[s_{j-1}(k) - s_j(k) \right]}{s_j(k) + \varepsilon} \\ U(s_j(k)) & = \begin{cases} v_f - s_{cr} \cdot \frac{v_f - v_{cr}}{s_j(k)}, & \text{if } s \geq s_{cr} \\ v_{cr} \cdot \frac{s_j(k) - s_{jam}}{s_{cr} - s_{jam}}, & \text{otherwise} \end{cases} \end{cases} \quad (10)\ (11)\ (12)$$

Eq. 10 is the discrete Lagrangian conservation equation, Eq. 11 is the discrete Lagrangian dynamic speed equation and Eq. 12 is the Lagrangian Smulders' fundamental diagram, which could also be other valid forms.

The proposed discrete dynamic speed equation (Eq. 11) has four components on the right-hand side. The first component is the current speed, the second component represents the influence of the difference between the desired speed and the current speed, the third component represents the influence of the speed of the front vehicle group, and the last component represents the influence of the spacing of the front vehicle group. The last three components together state that the drivers' desire to reach the equilibrium speed and the influences from the leading vehicles result in the finite acceleration/deceleration (i.e., the gradual change of speed) from the current speed. In contrast, the first-order model determines the speed purely by the spacing of the current vehicle group during the same time step. Obviously, the dynamic speed equation is more realistic according to the real-world observations.

The model has three additional critical parameters, i.e., τ, $\lambda(\theta)$, and ε. ε is added to ensure the computation stability, while τ and $\lambda(\theta)$ have physical meanings. τ represents the reaction delay time, and θ represents how much the current vehicle group is influenced by the front spacing condition. Thus, with a larger τ and a smaller θ, one may expect less sensitivity of the drivers to the front condition and more oscillations in congestions. This expectation is observed in the simulation results in Sec. 4.

This discrete model can be viewed as a state space model, and the state variables are the spacing and speed of the vehicle groups. This formulation makes it convenient to conduct joint estimation of speed and to incorporate vehicle speeds as measurements.

Influence of merges and diverges

The model described by Eq. 10-12 is a freeway link model, i.e., it does not take into considerations of the ramp flows. Van Wageningen-Kessels (*2*) has shown that with merge (onramp) flows and diverge (offramp) flows, the Langrangian conservation equation becomes:

$$\frac{\partial s}{\partial t} - \frac{\partial u}{\partial n} = -s^2 \cdot (\alpha - \beta). \tag{13}$$

Where α and β stands for the inflow rate and outflow rate (in $\mathrm{veh}/(\mathrm{m}\cdot\mathrm{s})$), respectively. The ramp flows can indirectly influence the mainstream speed through this conservation equation. However, the dynamic speed equation also needs to be modified to directly reflect the influence of ramp flows. Generally, the onramp flow merges into the mainstream flow with a lower speed $v_{onramp} < v_{main}$ and need to accelerate to match the mainstream speed. For the offramps, the exiting flow needs to decelerate to match the offramp speed limit. Thus both merge and diverge cause speed reduction in the mainstream flow. Previously, an additional term to the dynamic speed equation has been proposed (*9*) in the Eulerian second-order models to reflect this acceleration/deceleration phenomenon. For onramps it is described as $(v_{onramp} - v) \cdot \alpha / \rho$. Assume $v_{onramp} = (1-\upsilon) \cdot v$, it becomes $-\upsilon \cdot v \cdot \alpha / \rho$, $\upsilon \in [0,1]$. For offramps it is a similar term with α replaced by β. For the Lagrangian dynamic speed equation, a similar term can be added to Eq. 9 with ρ replaced by s, described in Eq. 14.

$$\frac{\partial u}{\partial t} = -\frac{\partial u}{\partial n} \cdot \frac{u}{s} + \frac{1}{\tau} \cdot \left[U(s) - u - \frac{\lambda}{s} \cdot \frac{\partial s}{\partial \mathrm{n}} \right] - (\upsilon_\alpha \cdot \alpha + \upsilon_\beta \cdot \beta) \cdot v \cdot s \tag{14}$$

The additional term represents the acceleration/deceleration phenomenon, which is in unit of m/s^2.

Boundary Conditions

The model is not completed for discrete simulation without appropriate boundary conditions. For the inflow boundary the minimum supply-demand method is applied (Eq. 15) (*16*). Let D_i stand for the demand of traffic flow in freeway segment i, and S_i the supply. Let q_{cr} stand for the critical flow. The time step index k is omitted for simplicity. The minimum supply-demand method for the inflow boundary is the same as that for the Eulerian case except for that the freeway segment i is in fact the available space in the most upstream, i.e., the distance between the starting position of the freeway and the position of the last vehicle group that is already in the computation domain. segment $i-1$ is a dummy segment where the unsatisfied traffic demand

queues. Once the calculated flow $q_{(i-1\to i)}$ is as large as a vehicle group of size Δn, it is allowed to enter the computation domain.

$$q_{(i-1\to i)} = \min D_{i-1},\ S_i$$

$$\begin{aligned} D_i &= \begin{cases} q_i & \text{if free flow}, s_i > s_{cr} \\ q_{cr} & \text{o.w.} \end{cases} \\ S_i &= \begin{cases} q_{cr} & \text{if free flow}, s_i > s_{cr} \\ q_i & \text{o.w.} \end{cases} \end{aligned} \tag{15}$$

At the outflow boundary, a dummy vehicle group is assumed to represent the out-boundary condition. The first vehicle group within the computation domain follows the dummy vehicle group according to the upwind method until it leaves the computation domain and becomes the new dummy vehicle group.

Stability Requirements

For the discrete simulation of the first-order Lagrangian model, the Courant-Friedrichs-Lewy's (CFL) condition described in Eq. 16 ensures the numerical computation stability.

$$\frac{T}{\eta_{\min}} \cdot \max \left| \frac{\partial U(s_j(k))}{\partial s} \right| \le 1 \tag{16}$$

Indeed, it limits the maximum distance that a vehicle group can travel within one time step. For detailed explanation we refer to (*2*). The minimum size of vehicle groups per lane ($\eta_{\min}$) is obtained by letting CFL=1. However, the second-order model incorporates a dynamic speed equation, and thus the CFL number cannot be approximated using Eq. 16. The condition is in fact the same that during one time-step, a vehicle group cannot cross two discretization boundaries in the numerical computation. Experimental experience from simulation found that the required vehicle group size is larger but still reasonable for a macroscopic level simulation.

Discussions

Arguments between the first-order models and the second-order models have never stopped. As mathematical models are approximations of the physical world, they can hardly be exactly accurate. The same is true for the Lagrangian traffic flow models. There is no simple conclusion for the comparison, as they both have their own advantages and disadvantages. The fundamental diagram is only a coarse approximation of the empirical evidence. The proposed model is more sensible as it improves the first-order model by dynamically modeling the speed. Particularly, the speed property would be related to vehicle groups instead of a location on the road. This makes the Lagrangian second-order model more reasonable than the Eulerian counterpart.

4 EXPERIMENTAL ANALYSIS

This section presents the experimental analysis of the proposed second-order model using a lane-drop scenario shown in Fig. 1. This experimental analysis is not intended to be a quantitative measure of how accurate the model is compared with a real data set. Rather, it is compared with the outputs of the first-order Lagrangian model to show the performance and the potential advantages of the second-order model, with the underlying assumption that the first-order model is reasonable (*2*).

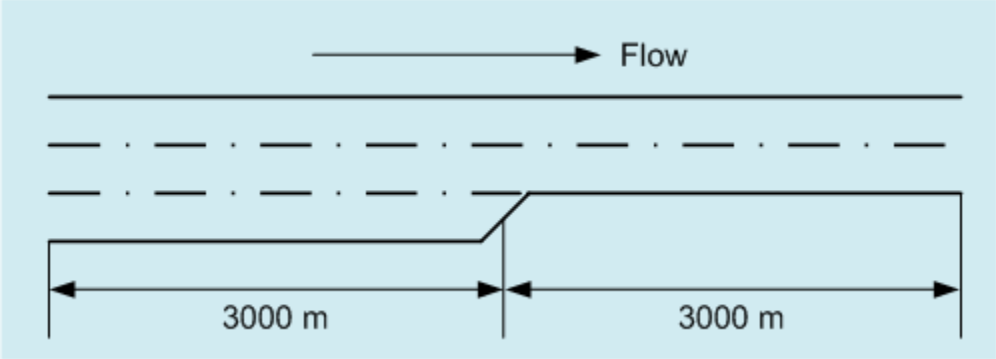

FIGURE 1 Experiment Scenario

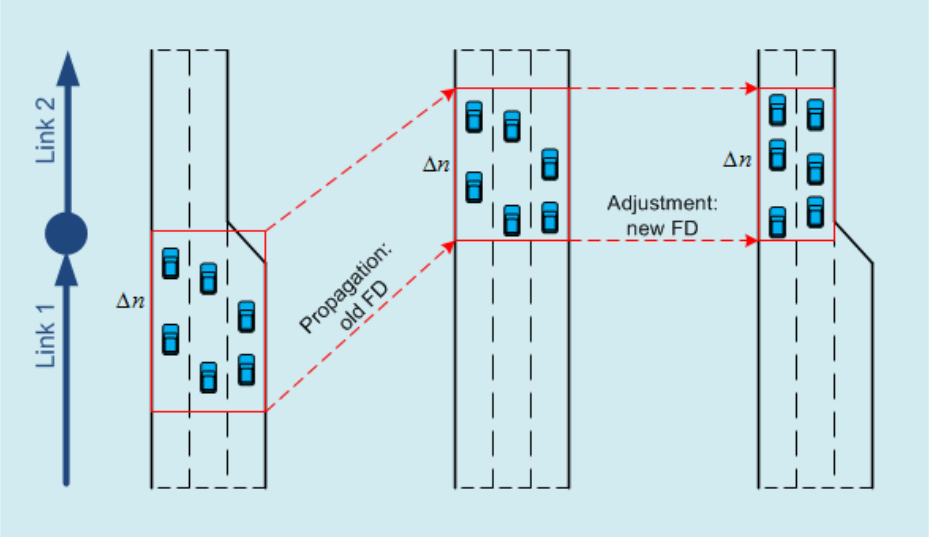

FIGURE 2 Lane-Drop Simulation Model

Scenario Description

A lane-drop scenario (Fig. 1) is assumed to emulate the onset and discharge of congestion. The total length of the freeway stretch is 6km without ramps. At $x = 3\text{km}$ the number of lanes drops from three to two. The initial condition is set to be low flow. Later on, a surge occurs in the inflow demand, which forms the congestion when it reaches the lane-drop area. The congestion propagates backward until the demand surge ends and the inflow queue disappears, and then it discharges, leaving a triangular shape of low speed area in the speed map.

Lane-Drop Simulation Model

To realize the lane-drop scenario in discrete simulation, the simulation model explained in Fig. 2 is adopted. When a vehicle group approaches the lane merging area, it is propagated ahead in the flow direction in an assumed three-lane freeway, and then the traffic characteristics (spacing, speed) are adjusted by assuming that the occupied area is the same while the number of lanes is reduced from three to two. The new spacing is calculated as $s_j^{k,new} = s_j^{k,old} \cdot (L_2 / L_1)$, where L_1 represents the number of lanes before the lane-drop, and L_2 represents the number of lanes after the lane-drop.

Experiment Settings

The Smulders' fundamental diagram is adopted, and the related parameters v_{cr} , v_f , s_{cr} , and s_{jam} are set to be 75km/h, 120km/h, 30m/veh/lane, and 5m/veh/lane. The simulation duration is 0.8h to allow a full evolution of congestion, and the demand surge occurs between 0.1h and 0.3h. The low-demand input flow is 1veh/second, while the high-demand input flow is 2veh/second. The time-step duration T is set to be 1 second, and the vehicle group size Δn is 4.6. For a first order model, the CFL condition requires that $\Delta n > 2.5$ with $T = 1$. Both the first-order model and the second-order model are implemented in MATLAB. All these settings are the same for both models to make the outputs comparable.

The second-order model has three more parameters to calibrate, namely, τ , θ (or λ), and ε . Two nominal sets are tested, where Set-1 uses $\tau = 1.05$, $\theta = 0.55$, and $\varepsilon = 0.05$, and Set-2 uses $\tau = 1.14$, $\theta = 0.40$, and $\varepsilon = 0.05$. At this point, the parameter sets for the dynamic speed equation are chosen to ensure the simulation stability and yield reasonable (in the sense of traffic flow dynamics) outputs given other foregoing settings. They are not optimized towards a real data set. On the other hand, it is noticed that given other foregoing conditions, the parameters τ , θ , and ε can only vary within a small range while the simulation is still stable. Thus one may expect that these parameters do not change greatly from the nominal data sets even when they are calibrated towards a real data set.

Outputs and Discussion

The simulation results are presented in Fig. 3 to Fig. 8. Fig. 3 shows the speed map for the first-order model, with an amplified area shown in the Fig. 4. Fig. 5 and Fig. 7 show the results for the second-order model with different parameter sets, with the same area amplified in Fig. 6 and Fig. 8, respectively. The lane-drop location and the amplified area are indicated in the figures. Initially, the demand volume is low such that the speed is close to the free flow speed, shown as the deep blue color. Between 360s and 1080s, the demand volume is increased, resulting in a lower speed shown as light blue color before the lane-drop. As the plotting area is truncated at $x = 1000m$, this high demand period is slightly shifted to the right in the figures. The increased inflow volume creates the congestion as it reaches the land-drop location (the bottleneck), and

the congestion propagates backward. When the inflow demand is decreased and the inflow queue is dissolved, the congestion begins to discharge.

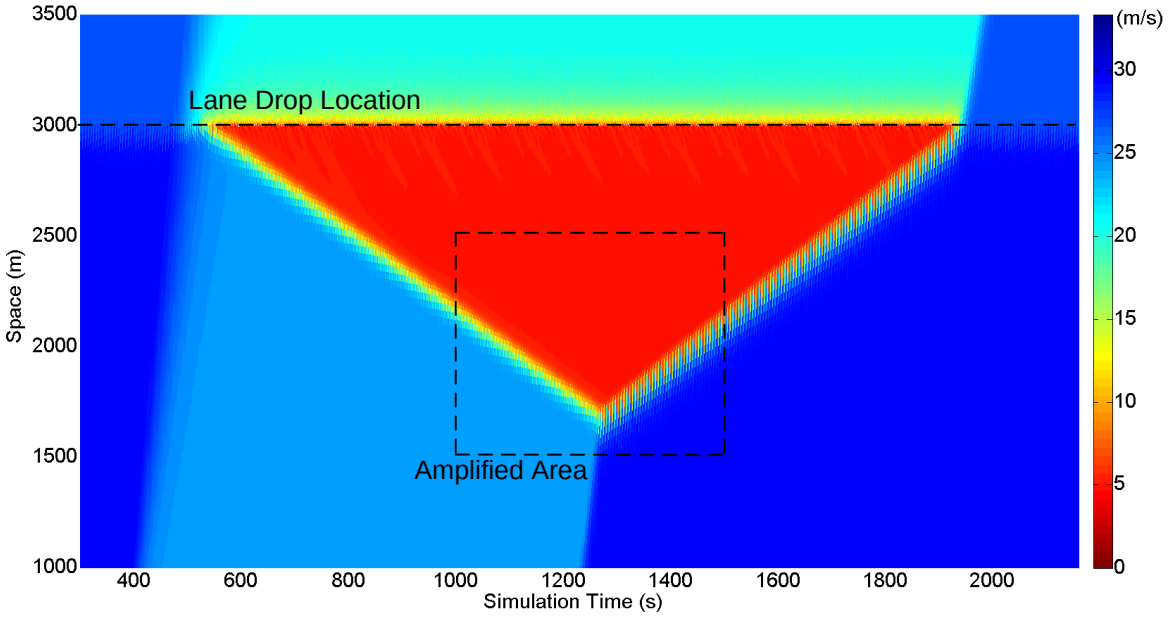

FIGURE 3 Speed Map: First-Order Model

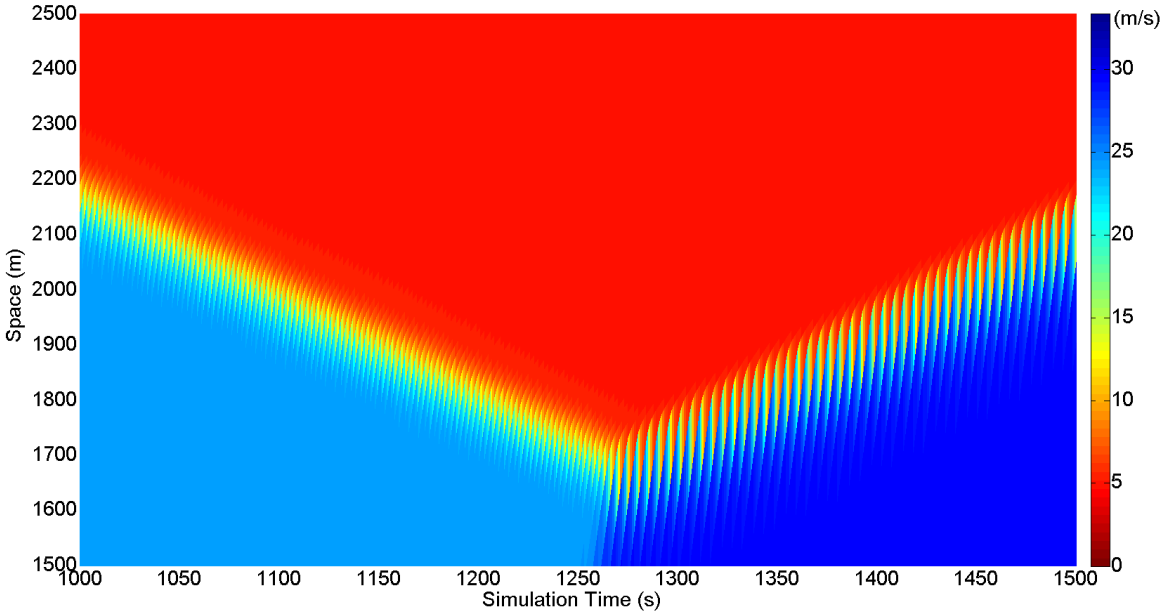

FIGURE 4 Speed Map – Amplified Area: First-Order Model

We can see from the figures that all of them are able to reproduce the onset and discharge of the congestion caused by the lane-drop bottleneck. However, these figures have observable differences. Fig. 5 exhibits similar pattern to that of the first-order model (Fig. 3) but with some slight oscillations of speed, while Fig. 7 shows more stop-and-go waves during the congestion.

These stop-and-go waves are amplified towards the bottom of the congestion triangle. Researchers have found similar patterns in analyzing the real world data (*17*).

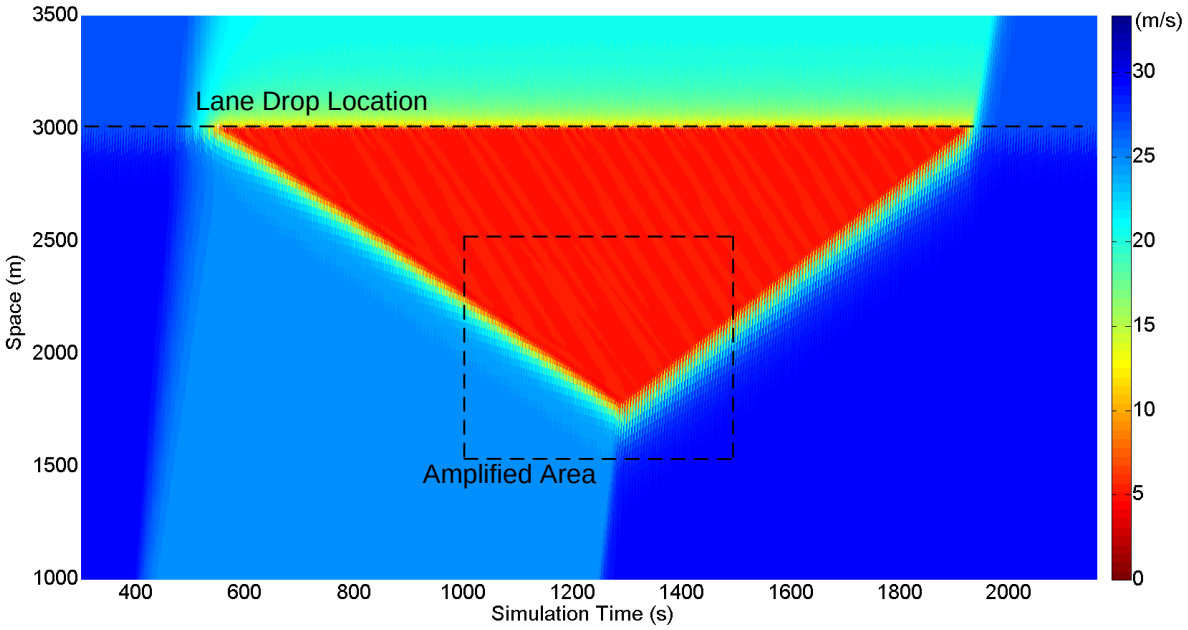

FIGURE 5 Speed Map: Second-Order Model with Parameter Set 1

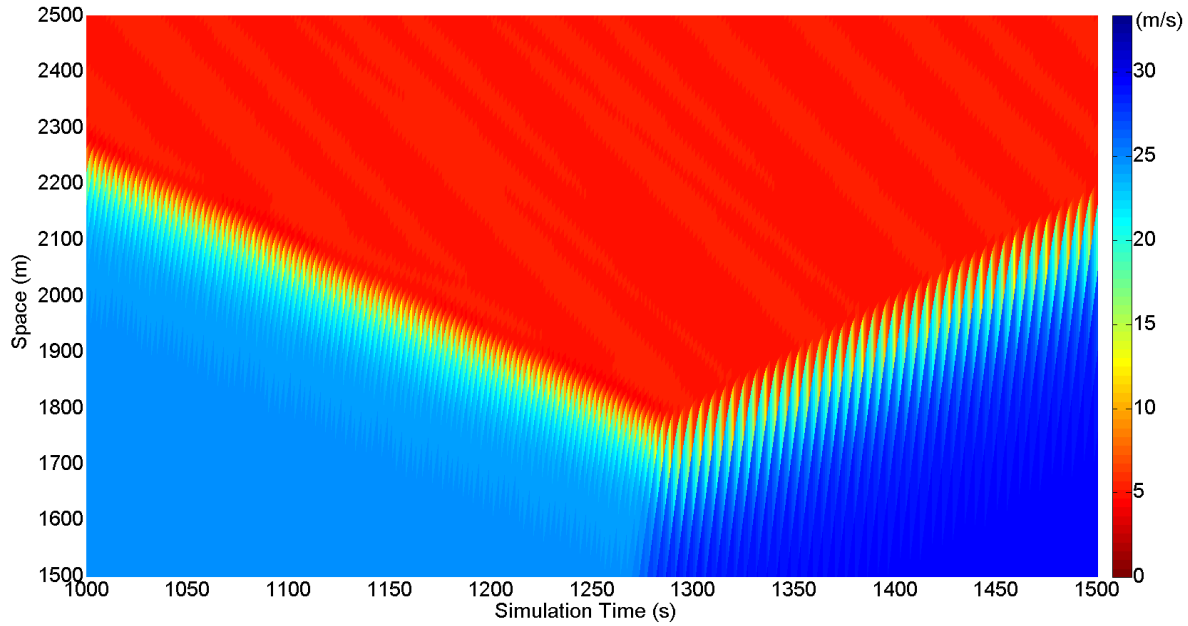

FIGURE 6 Speed Map – Amplified Area: Second-Order Model with Parameter Set 1

Van Wageningen-Kessels (*2*) has analyzed the stop-and-go waves that sometimes (e.g., low discretization resolution or CFL=1) appear in the first-order Lagrangian model, and concluded that those waves are artificial as they are resulted from the diffusion error, and should not be confused with the real-world stop-and-go waves. However, the second-order model naturally

creates the stop-and-go waves in congestion by adjusting how much the speed at current time-step relies on the speed during the last time-step, how fast it can reach the equilibrium speed, and how sensitive it is to the condition of the leading vehicles. When the reaction delay is relatively long, or that the vehicles are not sensitive to the front condition, the oscillation becomes more obvious (parameter Set-2). In the contrary, when the drivers reach their desired speeds faster and are more sensitive to the front conditions (parameter Set-1), the speed map becomes smoother. The resulted differences from the two parameter sets show the flexibility of the proposed model.

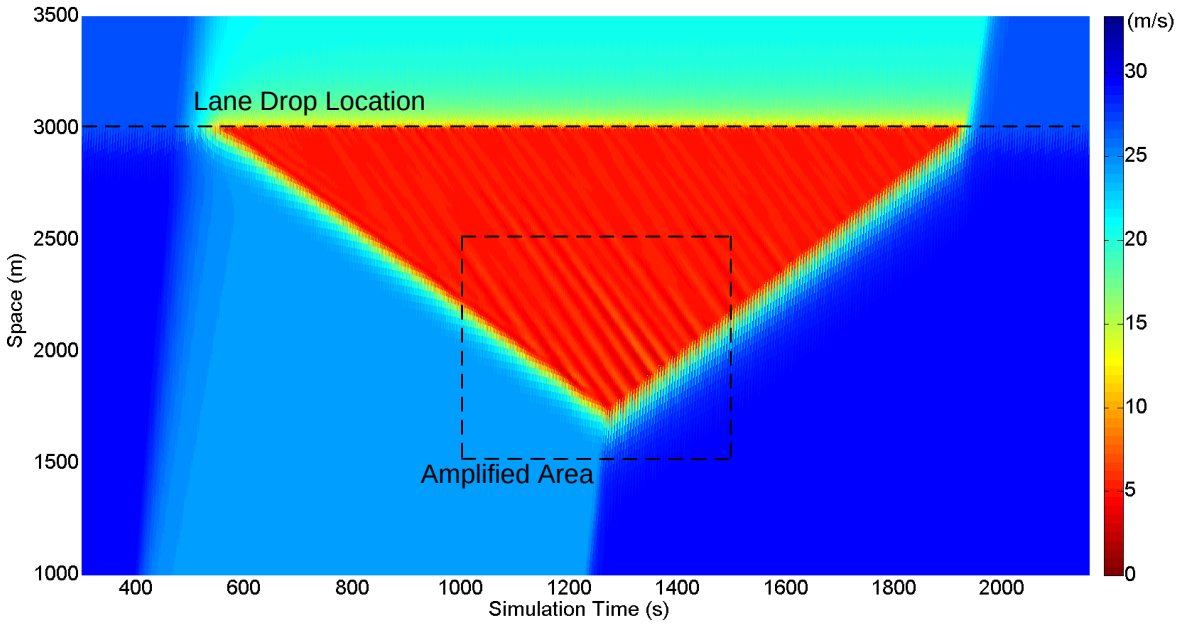

FIGURE 7 Speed Map: Second-Order Model with Parameter Set 2

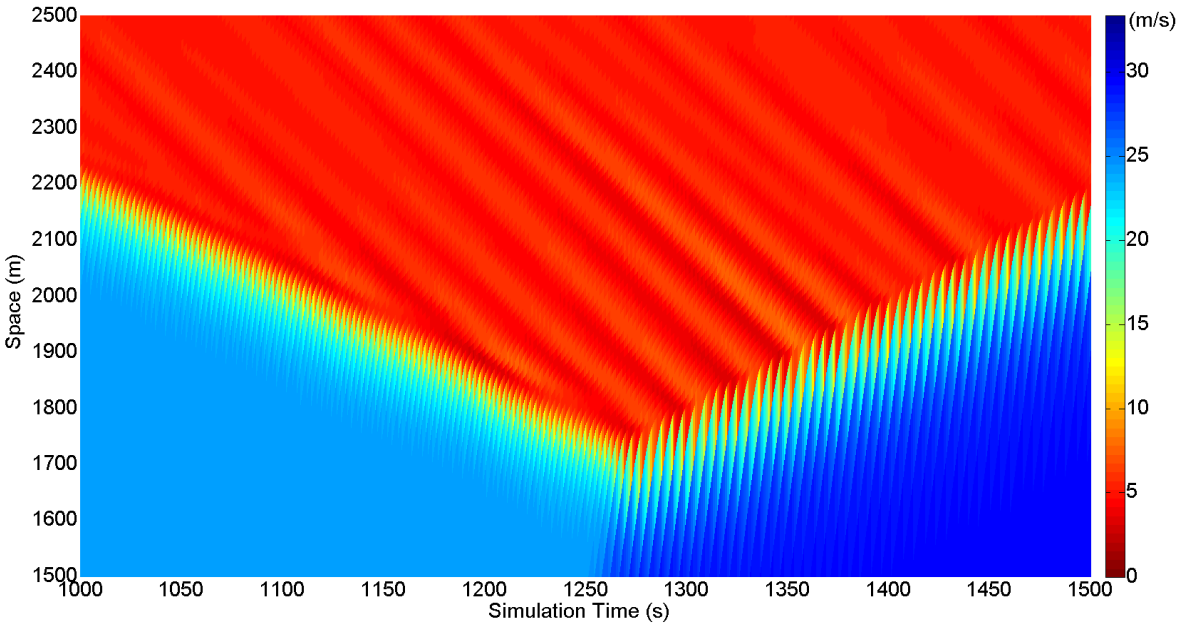

FIGURE 8 Speed Map – Amplified Area: Second-Order Model with Parameter Set 2

It is worth mentioning that the magnitude of the time delay parameter τ is one order higher than the drivers' reaction time in the microscopic level. In fact, this τ is two orders higher than the drivers' reaction time in the Eulerian case. It should be treated as a macroscopic parameter, rather than being enforced to be the microscopic one.

5 CONCLUSIONS

In this paper, we propose a second-order Lagrangian macroscopic traffic flow model. A dynamic speed equation is derived from the realistic modeling of the reaction delay and driving anticipation. We show in a lane-drop simulation that the second-order model is not only able to reproduce the onset and discharge of congestion as the first-order model does, but also able to naturally create stop-and-go waves which are amplified as the waves propagate backward. These phenomena are coincident with the patterns identified in the real-world data. In addition, it can facilitate joint estimation of speed and incorporating speed measurements in traffic state estimation. All these observations show that the proposed model has advantages over the first-order model. However, there are still some fundamental topics that are not addressed. For example, no empirical validation has been conducted even for the first-order model. Calibration of model parameters would be another worthwhile future work. We are continuing our efforts in this direction.

REFERENCES

1. Leclercq, L., J. A. Laval, and E. Chevallier. The Lagrangian coordinates and what it means for first order traffic flow models. In *Transportation and Traffic Theory 2007. Papers Selected for Presentation at ISTTT17*, 2007.
2. Van Wageningen-Kessels, F., Y. Yuan, S. P. Hoogendoorn, H. Van Lint, and K. Vuik. Discontinuities in the Lagrangian formulation of the kinematic wave model. *Transportation Research Part C: Emerging Technologies*, Vol. 34, 2013, pp. 148-161.
3. Payne, H. J. Models of freeway traffic and control. *Mathematical models of public systems*, Simulation councils, Inc., 1971.
4. Lighthill, M. J., and G. B. Whitham. On kinematic waves. II. A theory of traffic flow on long crowded roads. *Proceedings of the Royal Society of London. Series A. Mathematical and Physical Sciences*, No. 229(1178), 1955, pp. 317-345.
5. Richards, P. I. Shock waves on the highway. *Operations Research*, Vol. 4(1), 1956, pp. 42-51.
6. Daganzo, C. F. The cell transmission model: A dynamic representation of highway traffic consistent with the hydrodynamic theory. *Transportation Research Part B: Methodological*, Vol. *28*(4), 1994, pp. 269-287.
7. Daganzo, C. F. The cell transmission model, part II: network traffic. *Transportation Research Part B: Methodological*, Vol. *29*(2), 1995, pp. 79-93.
8. Newell, G. F. A simplified theory of kinematic waves in highway traffic, part I: general theory. *Transportation Research Part B: Methodological*, Vol. *27*(4), 1993, pp. 281-287.

9. Papageorgiou, M., J. M. Blosseville, and H. Hadj-Salem. Macroscopic modelling of traffic flow on the Boulevard Périphérique in Paris. *Transportation Research Part B: Methodological*, Vol. *23*(1), 1989, pp. 29-47.
10. Wang, Y., and M. Papageorgiou. Real-time freeway traffic state estimation based on extended Kalman filter: a general approach. *Transportation Research Part B: Methodological*, Vol. *39*(2), 2005, pp. 141-167.
11. Daganzo, C. F. Requiem for second-order fluid approximations of traffic flow. *Transportation Research Part B: Methodological*, Vol. *29*(4), 1995, pp. 277-286.
12. Paveri-Fontana, S. L. On Boltzmann-like treatments for traffic flow: a critical review of the basic model and an alternative proposal for dilute traffic analysis. *Transportation Research*, Vol. *9*(4), 1975, pp. 225-235.
13. Papageorgiou, M. Some remarks on macroscopic traffic flow modelling. *Transportation Research Part A: Policy and Practice*, Vol. *32*(5), 1998, pp. 323-329.
14. Smulders, S. Control of freeway traffic flow. *Ph.D. Dissertation, University of Twente, Enschede, The Netherlands*, 1989.
15. Yuan, Y., J. W. C. Van Lint, R. E. Wilson, F. van Wageningen-Kessels, and S. P. Hoogendoorn. Real-time Lagrangian traffic state estimator for freeways. *Intelligent Transportation Systems, IEEE Transactions on*, Vol. *13*(1), 2012, pp. 59-70.
16. Lebacque, J. P. The Godunov scheme and what it means for first order traffic flow models. In *Internaional symposium on transportation and traffic theory*, 1996, pp. 647-677.
17. Zielke, B. A., R. L. Bertini, and M. Treiber. Empirical measurement of freeway oscillation characteristics: an international comparison. *Transportation Research Record: Journal of the Transportation Research Board*, No. *2088*(1), Transportation Rsearch Board of the National Academies, Washington, D.C., 2008, pp. 57-67.